HHS Public Access

Author manuscript

Am Nat. Author manuscript; available in PMC 2016 March 01.

Published in final edited form as:

Am Nat. 2015 March ; 185(3): 332–342. doi:10.1086/679734.

Evolution of Pathogen Virulence Across Space During an Epidemic

Erik E. Osnas[1,2], **Paul J. Hurtado**[3,4], and **Andrew P. Dobson**[1]

Erik E. Osnas: erik.osnas@gmail.com; Paul J. Hurtado: hurtado.10@mbi.osu.edu; Andrew P. Dobson: dobson@princeton.edu

[1]Department of Ecology and Evolutionary Biology, Princeton University, Princeton, NJ 08544, USA

[2]Current Address: Patuxent Wildlife Research Center, United States Geological Survey, Laurel, MD 20708, USA

[3]Mathematical Biosciences Institute, The Ohio State University, Columbus, OH 43210, USA

[4]Department of Evolution, Ecology & Organismal Biology, The Ohio State University, Columbus, OH 43210, USA

Abstract

We explore pathogen virulence evolution during the spatial expansion of an infectious disease epidemic, in the presence of a novel host movement trade-off, using a simple spatially explicit mathematical model. This work is motivated by empirical observations of the *Mycoplasma gallisepticum* invasion into North American House Finch (*Haemorhous mexicanus*) populations; however, our results likely have important applications to other emerging infectious diseases in mobile hosts. We assume that infection reduces host movement and survival, and that across pathogen strains the severity of these reductions increases with pathogen infectiousness. Assuming these trade-offs between pathogen virulence (host mortality), pathogen transmission, and host movement, we find that pathogen virulence levels near the epidemic front (that maximize wave speed) are lower than the virulence level with a short-term growth rate advantage or that ultimately prevails (i.e., are evolutionarily stable) near the epicenter and where infection becomes endemic (i.e., that maximizes the pathogen basic reproductive ratio). We predict that, under these trade-offs, less virulent pathogen strains will dominate the periphery of an epidemic, and that more virulent strains will increase in frequency after invasion where disease is endemic. These results have important implications for observing and interpreting spatio-temporal epidemic data, and may help explain transient virulence dynamics of emerging infectious diseases.

Keywords

trade-off; invasion; movement; house finch; mycoplasma

Correspondence to: Erik E. Osnas, erik.osnas@gmail.com.

Introduction

A major insight from theoretical epidemiology that explains a large body of empirical observations is that parasites and pathogens are not expected to evolve low virulence levels if there is pathogen strain competition within hosts or a trade-off between a strain's transmission potential per unit time and it's infectious lifespan within a given host (Levin and Pimentel 1981; Anderson and May 1982; Bull 1994; Frank 1996; Day 2001, 2003; Day and Proulx 2004; Alizon et al. 2009). That is, if pathogens exploit their hosts in such a way that increased transmission leads to increased host mortality, then the ultimate outcome of pathogen evolution will be high or intermediate levels of virulence. Most of these theoretical results about virulence evolution are concerned with long term predictions of the evolutionarily stable virulence in a non-spatial population at equilibrium. However, many observations of disease in human, wildlife, or other systems are made during a spatially spreading epidemic, where short term dynamics of pathogen traits can be observed. Despite this fact, few theoretical investigations make short term predictions of virulence evolution (Lenski and May 1994; Day and Proulx 2004; André and Hochberg 2005; Day and Gandon 2006, 2007; Bolker et al. 2010), and the few that consider spatially structured populations are concerned with long term evolutionarily stable outcomes of virulence (Boots and Sasaki 1999; Haraguchi and Sasaki 2000; Boots et al. 2004).

One aspect that has not been well addressed is how pathogen virulence should change through space and time during an epidemic. During the emergence phase of an epidemic, the pathogen's range is expanding and it is plausible that the properties that lead to rapid spatial expansion might differ from those that maximize the instantaneous per capita growth rate of the infected class or that are the evolutionarily stable strategy (ESS) at equilibrium. Specifically, there might be a trade-off not only between transmission and virulence (disease-induced mortality, a component of the infectious period) but also between virulence and host (and therefore pathogen) movement, such as during migration or dispersal events.

A growing number of empirical examples provide additional motivation for examining the theoretical basis for short-term spatiotemporal virulence dynamics. In the Monarch butterfly, infection compromises host flying ability (Bradley and Altizer 2005) and populations that undergo more frequent or longer migrations are infected by pathogens with a lower average virulence (de Roode et al. 2008). In House Finches (*Haemorhous mexicanus*) infected with the bacteria *Mycoplasma gallisepticum*, infection causes individuals to lose dominance status and spend more time feeding at bird feeders (Hawley et al. 2007; Bouwman and Hawley 2010). In these birds, infection then may lead to less host-mediated pathogen dispersal but more transmission to hosts in a local area if transmission is associated with bird feeders. Moreover, virulence has decreased as the pathogen spread west from the introduction site of eastern North America but virulence increased subsequent to introduction in both eastern and western North America, as shown in Figure 1 (see Hawley et al. 2013). As has recently been reviewed (Altizer et al. 2011), host migration can act as a selective force that reduces pathogen prevalence and virulence; thus, if host movement or migration is blocked, higher prevalence and virulence might be maintained. These examples provide some evidence for the importance of changes in host movement due to infection on virulence evolution, yet we are not aware that this trade-off has been studied theoretically.

In order to examine the effect of infection-induced reduction in host movement on virulence evolution, and to make qualitative predictions about the spatiotemporal patterns of virulence evolution during the spatial spread of an emerging infectious disease, we used a simple deterministic reaction-diffusion model of a multi-strain epidemic when there are trade-offs between host movement and virulence and between transmission and virulence. We consider different pathogen strains advancing at various velocities through space. In simple diffusion models of population spread, the velocity of a spreading front (wave) is determined by the local growth rate of the spreading population, which for pathogens is determined by transmission and virulence rates, and by the spatial movement rates, which are determined by diffusion coefficients for infected hosts. After some initial establishment phase, the strains with higher velocity will advance ahead of other strains into a fully susceptible host population. Thus, two central questions of this paper arise: 1) assuming a trade-off between virulence and infected-host movement, how do strains with maximum velocity fair in competition against strains with a short-term growth rate advantage or strains that are evolutionarily stable at epidemic equilibrium? and 2) how does this competition play out at any particular location through time and along a moving wave front? We find that mean virulence can change quickly during an epidemic, that virulence levels near the periphery of a spatially spreading epidemic front can differ significantly from virulence levels in regions where disease is endemic, and we discuss the important implications of these results for observing and responding to epidemics and epizootics in real systems.

METHODS

The Model

We based our model on a spatially explicit model of susceptible (*S*) and infected (*I*) hosts (Liu and Jin 2007), here modified to include multiple pathogen strains:

$$\frac{\partial S}{\partial t} = D_S \nabla^2 S - \sum_i \beta_i I_i S - dS + \theta \quad (1a)$$

$$\frac{\partial I_i}{\partial t} = D_i \nabla^2 I_i + \beta_i I_i S - (d + \alpha_i) I_i \quad (1b)$$

Here, $S = S(x,t)$ is the density of susceptible hosts at location x at time t, and $I_i = I_i(x,t)$ is the density of hosts infected with pathogen strain i. The total population size at location x and time t is thus $N(x,t) = S + \Sigma_i I_i$. The operator ∇^2 is the second derivative with respect to spatial location, which for simplicity we consider to be the radial distance from the origin of the epidemic. Thus, $\nabla^2 I_i$ is the second derivative of strain i density with respect to location at time t. θ is a spatially and temporally constant inflow of susceptible hosts due to both immigration and birth, β_i is the transmission rate for strain i, d is the constant death rate that is common to both S and all I_i, and α_i is an additional amount of mortality for the hosts infected by strain i (hereafter, virulence of strain i). D_s and D_i are the diffusion coefficients for the S and I classes, respectively, and these are considered to be constant with respect to location and time, which is an important assumption that allows total diffusion to be affected

only by the second derivative with respect to location. Allowing the diffusion coefficient to vary with location is more realistic, but not necessary for the focus of this manuscript. In addition, we assume there is no mutation from strain *i* to strain *j*, a host can only be infected with one strain at a time, and that there is no disease recovery.

Model (1) does not have a known analytical solution, but numerical solutions can be found using standard computational techniques. However, Model (1) can be simplified defining a new variable that measures the density of S and I_i as a proportion of the density at the disease-free equilibrium, $N = \theta/d$. This gives the new variables $Q = Sd/\theta$ and $P_i = I_i d/\theta$. By recognizing that $P \approx 0$ and $Q \approx 1$ (i.e., $S \approx N$) at the front of the invasion, Model (1) can be approximated at the wave front with one equation for the prevalence of strain *i*

$$\frac{\partial P_i}{\partial t} = D_i \nabla^2 P_i + r_i P_i \quad (2)$$

with the initial growth rate of the infected population for strain *i* (hereafter the *initial fitness of strain i*) given by

$$r_{0,i} = \beta_i N - (d + \alpha_i). \quad (3)$$

This quantity (3) is clearly related to the basic reproductive ratio of the related non-spatial SI model, $R_{0,i}$, given by

$$R_{0,i} = \beta_i N / (d + \alpha_i). \quad (4)$$

While R_0 is often maximized by virulence evolution in non-spatial models, it is not always the case that selection maximizes R_0 (e.g., Boots et al. 2006; Cortez 2013). As we describe in greater detail below, and as suggested by (2), we here focus on the strain-specific $r_{0,i}$ values as these values are more clearly related to the selective forces driving the short-term evolutionary dynamics of interest. In general, after disease invasion when $P > 0$, strain fitness will be described by

$$r_i = \beta_i S - (d + \alpha_i). \quad (5)$$

This quantity (r_i) is analogous to the *effective reproduction number* for strain *i* suggested by (4), i.e., $R_{t,i} = \beta_i S(t)/(d + \alpha_i)$.

Equation (2) is known as the Skellam Equation (Skellam 1951; Kot et al. 1996). A key property of Equation (2) is that after an initial establishment phase where P_i may be less than a threshold for detection, a traveling wave for strain *i* will develop and eventually advance with velocity of

$$c_i = 2\sqrt{r_i D_i} \quad (6)$$

(Shigesada and Kawasaki 1997; Murray 2002).

We used the strain-specific wave speed (6) to understand the advance of pathogen strains into a naïve host population when there are trade-offs between virulence and transmission and between virulence and diffusivity (host movement). These trade-offs are motivated by considering that a pathogen must exploit its host to some degree and this exploitation has a cost, perhaps in terms of tissue damage or the host's immune response, that may reduce the survival rate and movement of the host. The transmission and diffusion phenotype were determined by the functions

$$\beta(\alpha)=\tau_0(1-e^{-\tau_1\alpha}) \quad (7)$$

for transmission, and

$$D(\alpha)=\sigma_0 e^{-\sigma_1\alpha} \quad (8)$$

for diffusion. Here τ_0 is the asymptotic contact rate, and τ_1 is a trade-off parameter that scales virulence to transmission. In equation (8), the parameter σ_0 set the baseline diffusion rate for avirulent pathogens, which is here the same as uninfected hosts, and σ_1 is the trade-off parameter for diffusion that determines how fast diffusion decreases toward zero with increasing virulence. These functions represent the upper limit of transmission or diffusion for a given level of virulence. Actual genotypic variation in a population may fall below these values, but we ignore this because selection will always favor higher transmission for a given level of virulence, and in the spatial dimension, strains with a higher diffusion coefficient will always have a higher wave speed for a given level of transmission and virulence. Thus, we only consider variation along these two constraint functions.

Model Simulation

To complement the analytical results we derived by assuming low prevalence ($P \approx 0$) along an expanding front, we also used numerical solutions of model (1) in order to understand how mean virulence changes across space and time as prevalence increases and strain fitness r_i (equation 5) is influenced by a reduction in susceptible density. We used the method of lines (Smith 1985) implemented in R (R Core Team 2013) using the package deSolve (Soetaert et al. 2010). We used 100 strains that varied in virulence phenotype (α) with equal spacing from 0 to 10, and we considered the wave speed of pathogen strains that differ in transmission (β) and diffusivity (D) along the two constraint functions (trade-offs) above (Equations 7 and 8). We then calculated the mean virulence at location x and time t as $\overline{\alpha}(x,t)=\sum_i \alpha_i I_i/I_T$, where $I_T = \Sigma_i I_i$. Each strain was introduced at a prevalence of 0.01%; thus, mean virulence at $x = 0$, $t = 0$ was 5. We compared mean virulence at the wavefront through time to the mean virulence through time at the point of introduction ($x = 0$). We defined the wavefront as the furthest point in space for which prevalence was > 1%, which we considered a reasonable threshold of detection.

RESULTS

We begin by describing how transmission, virulence and host movement trade-offs affect the rate of spread of an individual strain by describing how the strain's wave speed (c_i) is related to it's initial fitness ($r_{0,i}$) and infected-host movement parameter D_i. This is

important because the strain with the highest wave speed dominates the epidemic wave front, and thus drives virulence evolution on the leading edge of the epidemic. Assuming only a transmission-virulence trade-off (i.e., no movement-virulence trade-off) we show that maximizing wave speed (c) is equivalent to maximizing fitness (r). We then compare those optimal virulence levels on the wave front with those that arise when a movement-virulence trade-off is present in the model. We further examine the spatiotemporal virulence dynamics of model (1) numerically, comparing the behavior of the model in a classical sense (with the transmission-virulence trade-off but no movement-virulence trade-off) to the dynamics observed in the presence of both the transmission-virulence and movement-virulence trade-offs. We conclude the results section with an application of the Price Equation version of the model to help clarify the interpretation of our simulation results.

Spatial Virulence Dynamics

Assuming trade-off constraints for transmission and diffusion (Equations 7 and 8, respectively), and a parameter regime that yields a traveling wave solution to (1), then the strain-specific wave speed equation (6) becomes

$$c(\alpha)=2\sqrt{r_0(\alpha)D(\alpha)}, \quad (9)$$

the fitness equations (3) and (5) become

$$r_0(\alpha)=\beta(\alpha)N-(d+\alpha) \quad (10)$$

$$r(\alpha)=\beta(\alpha)S-(d+\alpha) \quad (11)$$

and the maximum wave speed $c_* \equiv c(a_*)$ is given by the virulence level a_* that satisfies $c'(a_*) = 0$ and $c''(a_*) < 0$. Differentiating $c(a)$ to find it's maximum gives

$$c'(\alpha)=\frac{c(\alpha)}{2}\left(\frac{r_0'(\alpha)}{r_0(\alpha)}+\frac{D'(\alpha)}{D(\alpha)}\right) \quad (12)$$

Equation (12) shows that the wave speed $c(a)$ is maximized where the relative slope of pathogen fitness $r_0(a)$ is equal in magnitude and opposite in sign to the relative slope of the diffusivity $D(a)$. Note that if there is no trade-off between virulence and host movement, then $D'(a) = 0$ and we recover the expected result for the transmission-virulence trade-off: the maximum wave speed will be attained by the most virulent pathogen that maintains $r_0(a) > 0$ and maximizes $r_0(a)$.

Figure 2 shows the relationship between virulence (a), wave speed (c), and fitness (r) under equations (7–9). When the diffusion coefficient declines with virulence, the wave speed for an advancing pathogen strain will have a maximum at a lower virulence than the virulence that maximizes local fitness r_0 (Figure 2a, b), and by equation (12) the magnitude of this effect can be quite large when the diffusion trade-off is strong.

Virulence Dynamics: Epicenter versus Wave Front

The virulence dynamics like those shown in Figure 3 are a compromise between the forces that in the short term maximize spatial spread (i.e., wave speed, $c(\alpha)$) with those that ultimately maximize local growth rate (i.e., fitness, $r(\alpha)$). Assuming no movement-virulence trade-off ($D(\alpha)$ constant), these are both equivalent to maximizing fitness $r_0(\alpha)$. However, with a movement-virulence trade-off ($D(\alpha)$ not constant), variation in virulence drives variation in both transmission and host movement. This leads to different virulence levels associated with the maximum wave speed $c(\alpha)$ and maximum fitness $r(\alpha)$, which can yield a different pattern of virulence evolution across space and time (Figure 3). The movement-virulence trade-off plays a major role in shaping these dynamics. Eventually, with or without a movement-virulence trade-off, the evolutionarily stable strain that comes to dominate at the endemic steady-state according to Model (1) is the strain which maximizes (4) in non-spatial models (simulation results not shown).

Figure 3a, shows the mean virulence dynamics assuming there is a trade-off between virulence and transmission but no movement-virulence trade-off (D constant). In this case, wave speed $c(\alpha)$ will be maximized when fitness $r(\alpha)$ is maximized, which is the classic condition for the short-term evolutionary advantage during an epidemic. Therefore, the strain with maximum velocity also has the short-term evolutionary advantage, and there is a substantial change in mean pathogen virulence over time but only a small spatial gradient in mean pathogen virulence (Figure 3a). When there is a trade-off between virulence and host movement (Figure 3b), mean virulence on the wave front is lower than the mean virulence at the epicenter at the same point in time. This difference in virulence dynamics is shown in Figure 4.

Two assumptions implicit in model (1) raise the question: How are the results above influenced by changes in population density? In particular, we have assumed a density-dependent transmission rate ($\beta_i IS$) that causes fitness (11) to depend on susceptible host density, and we have allowed population size to vary during epidemics by assuming disease increases mortality (from d to $d+\alpha$) and that inflow of new susceptible hosts is constant (rate θ). To address this question, we considered two variations of model (1): the first uses a frequency-dependent transmission rate ($\beta_i IS/(S + I)$) and the other maintains constant local population size by assuming that the inflow of new susceptible hosts exactly matches losses from movement and death. Neither model produced substantially different results from those presented above in the sense that mean virulence along the wave front was initially lower than at the epicenter (see Online Figures B1–B4, and the code to reproduce those figures, in the Online Supplement). In the frequency-dependent transmission case, however, there was a very steep spatial and temporal gradient in prevalence, and in mean virulence, that coincided with the wave front (Online Figure B1). This caused mean virulence along the wave front to initially be much lower than at the epicenter, but quickly increase to relatively high levels after the wave front passed (Figure B2). In the case where local population size was kept constant, we obtained a nearly identical qualitative pattern of mean virulence as model (1) (Online Figures B3–B4), suggesting that the mean virulence dynamics produced by model (1) are not heavily influenced by changes in population density.

The Price Equation Formulation

The Price Equation formulation of model (1) partitions the rate of change in average trait values into two factors: change due to local selective forces on transmission and change due to the movement of infected individuals. As detailed in Appendix A, we follow Day and Gandon (2006 Day and Gandon (2007) to transform model (1) into Price Equations form,

$$\frac{\partial \overline{z}}{\partial t} = \sigma_{z\beta} S - \sigma_{z\alpha} + \frac{m_T}{I_T}(\overline{z_m} - \overline{z}) \quad (13)$$

Here z is a strain-related quantity (either β, α, D or r). The local population mean of z is $\overline{z} = \sum_i q_i z_i$, where $q_i(x,t) = (I_i(x,t))/I_T$ is the proportion of infections from strain i with $I_T = \Sigma_i I_i$. The covariance of traits y and z is σ_{yz} (see Appendix A), the strain specific movement rate of infected individuals is $m_i = D_i \nabla^2 I_i$, the total movement rate is $m_T = \Sigma_i m_i$, and we denote the average trait value among those infected individuals that are moving into or out of a location with a subscript m, i.e., $\overline{z_m} = \sum_i z_i m_i / m_T$.

If we let $\overline{\mathbf{z}}$ be the column vector of mean trait values, $[\overline{\beta}, \overline{\alpha}, \overline{D}]'$ we can write (13) in terms of a genetic covariance matrix and selection vector $[S, — 1,0]'$, and a second term that is the product of the total per capita movement rate of infected individuals into (positive) or out of (negative) a given location, times the difference in average trait values between those moving individuals and the local population. This gives

$$\frac{\partial}{\partial_t}\begin{bmatrix} \overline{\beta} \\ \overline{\alpha} \\ \overline{D} \end{bmatrix} = \underbrace{\begin{bmatrix} \sigma_{\beta\beta} & \sigma_{\beta\alpha} & \sigma_{\beta D} \\ \sigma_{\beta\alpha} & \sigma_{\alpha\alpha} & \sigma_{\alpha D} \\ \sigma_{\beta D} & \sigma_{\alpha D} & \sigma_{DD} \end{bmatrix}\begin{bmatrix} S \\ -1 \\ 0 \end{bmatrix}}_{\text{Local Transmission}} + \underbrace{\frac{m_T}{I_T}\begin{bmatrix} \overline{\beta_m} - \overline{\beta} \\ \overline{\alpha_m} - \overline{\alpha} \\ \overline{D_m} - \overline{D} \end{bmatrix}}_{\text{Movement}} \quad (14)$$

Again following the population genetics approach of Day and Gandon, we interpret the individual variance terms σ_{zz} in (14) as direct effects of selection, and the covariance terms as indirect effects of selection. This leads to the following inferences: First, selection acts *directly* to 1) increase mean transmission in proportion to the size of the susceptible population S, and 2) to decrease virulence. Second, in the presence of a transmission virulence trade-off ($\sigma_{\beta a} > 0$) selection acts *indirectly* to increase virulence and decrease transmission. That tension between conflicting direct and indirect effects eventually results in the classic evolutionarily stable level of virulence, but only after passing though potentially very high mean virulence. Third, selection has a neutral (direct) effect on host movement (D), and only indirectly changes the mean diffusion rate $\overline{D}$ through transmission and virulence.

The relative contributions of transmission-related local selection (first term in (14)) and strain-dependent host movement (second term in (14)) on the virulence dynamics are more difficult to understand because both play a role simultaneously. Nonetheless, this Price Equation form (14) does provide some insight into the conditions for when one factor dominates the other. The second term in (14), $m_T/I_T(\overline{\mathbf{z_m}} - \overline{\mathbf{z}})$, describes how local average

trait values change in response to the movement of infected individuals into and out of a given location: it captures whether there is a net loss ($m_T < 0$) or gain ($m_T > 0$) of infected individuals, and whether those individuals have relatively higher $(\overline{\mathbf{z_m}} - \overline{\mathbf{z}} > 0)$ or lower $(\overline{\mathbf{z_m}} - \overline{\mathbf{z}} < 0)$ average trait values than the local population. When this second quantity is high (e.g., as one might expect it to be along the front) host movement dynamics should dampen local selection effects. On the other hand, *when per capita* net host movement rates are lower (e.g., near the epicenter or where disease is endemic), the local selection effect driven by the transmission virulence trade-off should dominate.

Discussion

Most virulence evolution theory concerns long term outcomes and until recently little theory has addressed short term dynamics of virulence (André and Hochberg 2005; Day and Gandon 2006, 2007; Alizon et al. 2009; Messinger and Ostling 2009; Bolker et al. 2010). This is probably due to the difficulty of observing short term dynamics of trait values in anything other than laboratory populations. In fact, there are very few examples of virulence evolution in a single population, let alone observations of trait dynamics unfolding over the spatial dimension. Often in wildlife or even human populations, disease detection or estimation of disease rates (prevalence or force of infection) is difficult enough, and estimating the trait values of circulating strains adds an additional level of difficulty that can rarely be justified except for important diseases with major public health consequences (i.e., influenza). However, as more researchers intensely observe and study new epidemics across large time and space scales, then observing changes in disease trait values may become more common. In this case, it is important to have a theoretic expectation for our hypotheses and observations. The model here is an attempt at making these predictions in the most simplified system possible.

The results presented here have several practical implications for the observation of spatial epidemics. First, and most obvious, is that we only expect to see a large spatial gradient in virulence (Figure 3) for pathogens that cause a strong reduction in host movement relative to the transmission-virulence trade-off. When there is no host movement (diffusion) cost of virulence, then only the strains near the maximum fitness will initially both increase in frequency and advance quickly through space. Eventually, those strains that are evolutionarily stable will come to dominate everywhere. Thus, in systems where a large host movement cost of virulence exists, the first strain detected along an invasion front will not likely represent the characteristics of the disease in other locations, nor will it represent the final trajectory of the evolutionary process. Whereas without host movement costs, only evolutionary (time) dynamics of trait values need to be considered. Second, in the presence of a spatial virulence gradient and where detection is dependent on visible symptoms that are correlated to virulence (Jennelle et al. 2007), disease detection at the wave front might be compromised by low virulence strains predominating along the wave front. In this case, the detection threshold for disease prevalence will be a function of strain or mean virulence. If only one strain is circulating at a time, then this would be equivalent to each strain having a different detection threshold that depends on virulence. Such a situation could lead to very complex spatial patterns of invasion that are difficult to interpret without explicit

quantitative models and measurement of disease traits (either the mean or strain-specific traits). An easier approach might be to use detection methods that do not suffer from such trait-based observation biases (i.e., random PCR screening rather than surveys for symptomatic cases).

A detection bias caused by a correlation between virulence and observation might also lead to problems in assigning cause to emerging epidemics. Often researchers detect a new virulent disease and assume that either the disease has recently emerged at that virulence or that something has changed in the host population to cause this increased virulence, for example changes in susceptibility or resistance mediated through immune function due to stress. The model presented here suggests a simple alternative, namely that the pathogen has evolved higher virulence *in situ* after an initial introduction of an avirulent, fast-spreading, less detectable strain. When studying traits of emerging pathogens, evolution of those traits should be expected for pathogens that can generate high levels of diversity very quickly (many viruses and bacteria) or that are initially genetically diverse. We hope this work encourages others think carefully about matching model assumptions with system-specific knowledge of factors that shape the evolution of virulence (or other traits), and to keep various alternatives in mind when interpreting observed patterns of virulence and epidemic dynamics.

It may seem that the presence of a movement-virulence trade-off (i.e., a negative correlation between infected-host movement rate parameters D_i and parasite virulence α_i), combined with a virulence decrease on the margins of a spreading epidemic, would increase $\overline{D}$ and thereby increase the epidemic wave speed. However, as suggested by equation (6), whether or not a transient increase in $\overline{D}$ causes the epidemic wave speed to increase depends on how the virulence dynamics change mean local fitness (i.e., the net growth rate of the infected class), $\overline{r}$. Therefore, we do expect these evolutionary dynamics to yield non-constant epidemic wave speeds, but these may be accelerating or decelerating (see Figures 3, and Online Figures B1–B4).

The model presented here was motivated by empirical observations of the bacterial pathogen *Mycoplasma gallisepticum* invading into House Finch populations across North America (Figure 1; Hosseini et al. 2006; Dhondt et al. 2006; Hawley et al. 2013). In this system, the spread of the pathogen just after discovery in eastern North America matched a diffusion model very closely (Hosseini et al. 2006). Subsequently, when the pathogen was found in western North America, prevalence was lower and severe population effects on the finch were not noted in the west as they were in the east (Hochachka and Dhondt 2000; Dhondt et al. 2006). It was hypothesized that the western finch populations were more resistant to the pathogen (Hawley et al. 2005) but laboratory measurement showed that the pathogen isolates in the west were of lower pathogenicity than the original or subsequent eastern pathogen isolates (Figure 1; Hawley et al. 2010; Grodio et al. 2012; Hawley et al. 2013). Because host survival (virulence) is reduced with disease symptoms (Faustino et al. 2004), the lower pathogenicity of the western strains reflect lower virulence and a geographic cline in pathogen virulence. Moreover, observation of infected birds in this system suggested that infected birds also reduce movement (Hawley et al. 2007) and dominance at feeders (Bouwman and Hawley 2010). The model here is an attempt to make qualitative predictions

for virulence evolution when there is a host movement cost to virulence, and the results of the model are consistent with a movement cost to virulence in House Finches with subsequent increasing virulence after the pathogen has invaded a local finch population. Our model predicts that virulence will increase in areas that have been invaded recently (e.g., California) since there is a strong positive covariance between transmission and virulence across strains (Hawley et al. 2013; Williams et al. 2014). However, any increase in virulence in the finch system or any other system should not be taken as evidence for evolution proceeding directly toward a high evolutionarily stable virulence; instead, short term advantages to high transmission rate could alone drive virulence very high (Figure 3 and 4, also see Day and Gandon 2007), i.e., transient virulence dynamics do not necessarily move monotonically towards an evolutionarily stable virulence.

The present results refer to continuous and homogeneous space with diffusive movement outward from the introduction point. However, many wildlife systems exhibit seasonal movement or migration events (Altizer et al. 2011). While the model does not directly incorporate this periodic movement, our predictions likely still apply to such situations. Seasonal movement or migration can be viewed as periods of alternating stasis (no diffusion) and movement (increased diffusion). This type of dynamic predicts that, during periods of no movement, evolution will increase transmission and eventually move towards an evolutionarily stable virulence, while during migration evolution will lower virulence along the wavefront, assuming these trade-offs are present. In the results shown here (Figure 3), this implies increasing virulence during times of stasis and decreasing virulence as the population migrates through space when there are strong movement costs to virulence. However, the trade-off functions themselves may vary through the seasons, either due to intrinsic host reasons or due to changes in the external environment, and these more complicated mechanisms deserve study for the effect on virulence evolution. Ultimately, if migration is essential to either escape regions that are uninhabitable for part of the year, or to ensure enhanced breeding success, then migration will tend to select for reduced levels of virulence.

Adding more realism to our model (host recovery, mutation between pathogen strains, various dispersal kernels, a heterogeneous environment, explicit stochastic dynamics, or explicit genetic trait architecture) could prove insightful. The importance of these additions on expectations for virulence evolution can only be judged in reference to the simplest process possible, which is presented here. Our initial investigation of deterministic mutation (not shown) revealed no substantive difference from the results presented here, although mutation rate did affect the rate of mean trait evolution just as expected from basic principles. Stochastic drift and mutation coupled to the trade-offs modeled here might prove useful, but also will greatly blur the underlying deterministic process and predictions (André and Hochberg 2005; Travis et al. 2007, 2010). One important implication of stochastic drift and mutation in space will be the creation of long tendrils of non-adaptive trait values developing through regions of space (“mutational surfing”, Travis et al. 2007, 2010). In any case, considering stochastic processes is essential for interpreting data under alternative models, represents an alternative hypothesis to the selective processes we have modeled here, and should be considered when interpreting spatiotemporal trait dynamics. This non-selective alternative probably represents the normal expectation when studying emerging

infectious disease but might be tested by measuring movement costs of virulence (or other processes that may correlate to virulence), and these movement costs might prove more easily measured experimentally or observationally than the precise functional form of the transmission-virulence trade-off (e.g., Bradley and Altizer 2005).

We have applied this model and ideas to disease pathogens, however, we believe that analogous processes must operate in invasive species that exhibit trade-offs between important traits determining competition and colonization success and either generate high levels of genetic diversity after introduction or are introduced with large population sizes and high genetic diversity (Lee 2002, 2010). In general, the trait values measured along the advancing wave of the organism may be very different than the trait value that gives a persistence or transient advantage near the population center. In these cases, the underlying genetic architecture of the traits involved in trade-offs will have great influence over the potential for rapid spatiotemporal dynamics of the evolutionary process (Lee 2002; Lambrinos 2004; Hastings et al. 2005; Travis et al. 2007, 2010). That is, the structure of correlations and trade-offs between all of these traits, be they commonplace or system-specific, are an essential force shaping the spatiotemporal evolutionary dynamics of interest. Thus, when investigating both invasive species and emerging pathogens, considering hypotheses which include rapid evolutionary processes may provide valuable insights into observed and predicted patterns.

Supplementary Material

Refer to Web version on PubMed Central for supplementary material.

Acknowledgments

Discussion with Dana Hawley, Steve Ellner, Jim Murray, Troy Day, Colin Torney, Michael Cortez, and Joe Tien, and comments from two reviewers, improved this manuscript. Work was funded by NSF-EF Grant #0622705 to A. Dhondt under the NSF-NIH Ecology of Infectious Diseases program. P. Hurtado was supported by the Mathematical Biosciences Institute at OSU (NSF DMS #0931642). Partial support for A. Dobson was provided by NIH grant #R01GM085232 as part of the joint NIH-NSF-USDA Ecology and Evolution of Infectious Diseases program.

Appendix A Derivation of Price Equation

Here we derive the Price Equation form of model (1) following Day and Gandon (2006 Day and Gandon (2007). Writing (1) in terms of the frequency of each strain, $q_i(x,t) = I_i(x,t)/I_T(x,t)$, with $I_T = \Sigma_i I_i$, gives

$$\frac{\partial q_i}{\partial t} = q_i(r_i - \overline{r}) + \frac{D_i \nabla^2 I_i}{I_T} - q_i \frac{\sum_i D_i \nabla^2 I_i}{I_T}. \quad \text{(A1)}$$

The bar denotes the mean of a given value z (e.g., r, β, α, or D) across strains, $\overline{z} = \sum_i q_i z_i$.

Combining this with $\frac{d\overline{z}}{dt} = \sum_i z_i \frac{dq_i}{dt}$, the average trait value dynamics obey

$$\frac{\partial \overline{z}}{\partial t} = \sigma_{zr} + \frac{m_T}{I_T}(\overline{z}_m - \overline{z}) \quad \text{(A2)}$$

where $\sigma_{xy} = \overline{xy} - \overline{xy}$ denotes the covariance between traits x and y, $\overline{z}_m = \sum_i z_i \frac{m_i}{m_T}$ $m_i = D_i \nabla^2 I_i$, and $m_T = \Sigma_i m_i$. Substituting $r = \beta S - (d + \alpha)$ into the above expressions yields

$$\frac{\partial \overline{z}}{\partial t} = \sigma_{z\beta} S - \sigma_{z\alpha} + \frac{m_T}{I_T}(\overline{z}_m - \overline{z}) \quad \text{(A3)}$$

Letting $\overline{\mathbf{z}}$ be the column vector of mean trait values, $\overline{\mathbf{z}} = (\overline{\beta}, \overline{\alpha}, \overline{D})$, then

$$\frac{\partial \overline{\mathbf{z}}}{\partial t} = \begin{bmatrix} \sigma_{\beta\beta} & \sigma_{\beta\alpha} & \sigma_{\beta D} \\ \sigma_{\beta\alpha} & \sigma_{\alpha\alpha} & \sigma_{\alpha D} \\ \sigma_{D\beta} & \sigma_{D\alpha} & \sigma_{DD} \end{bmatrix} \begin{bmatrix} S \\ -1 \\ 0 \end{bmatrix} + \frac{m_T}{I_T} \begin{bmatrix} \overline{\beta}_m - \overline{\beta} \\ \overline{\alpha}_m - \overline{\alpha} \\ \overline{D}_m - \overline{D} \end{bmatrix}. \quad \text{(A4)}$$

References

Alizon S, Hurford A, Mideo N, Van Baalen M. Virulence evolution and the trade-off hypothesis: history, current state of affairs and the future. Journal of Evolutionary Biology. 2009; 22:245–259. [PubMed: 19196383]

Altizer S, Bartel R, Han BA. Animal Migration and Infectious Disease Risk. Science. 2011; 331:296–302. [PubMed: 21252339]

Anderson RM, May RM. Coevolution of hosts and parasites. Parasitology. 1982; 85:411–426. [PubMed: 6755367]

André JB, Hochberg ME. Virulence evolution in emerging infectious diseases. Evolution. 2005; 59:1406–1412. [PubMed: 16153027]

Bolker BM, Nanda A, Shah D. Transient virulence of emerging pathogens. Journal of The Royal Society Interface. 2010; 7:811–822.

Boots M, Hudson PJ, Sasaki A. Large Shifts in Pathogen Virulence Relate to Host Population Structure. Science. 2004; 303:842–844. [PubMed: 14764881]

Boots, M.; Kamo, M.; Sasaki, A. Disease Evolution: Models, Concepts and Data Analyses. Vol. 71. American Mathematical Society; 2006. The implications of spatial structure within populations to the evolution of parasites; p. 3-21.DIMACS Series in Discrete Mathematics and Theoretical Computer Science

Boots M, Sasaki A. 'Small worlds' and the evolution of virulence: infection occurs locally and at a distance. Proceedings of the Royal Society of London. 1999; 266:1933–1938.Series B: Biological Sciences

Bouwman KM, Hawley DM. Sickness behaviour acting as an evolutionary trap? Male house finches preferentially feed near diseased conspecifics. Biology Letters. 2010

Bradley CA, Altizer S. Parasites hinder monarch butterfly flight: implications for disease spread in migratory hosts. Ecology Letters. 2005; 8:290–300.

Bull JJ. Perspective: Virulence. Evolution. 1994; 48:1423–1437.

Cortez MH. When does pathogen evolution maximize the basic reproductive number in well-mixed hostâĂŞpathogen systems? Journal of Mathematical Biology. 2013; 67:1533–1585. [PubMed: 23070214]

Day T. Parasite Transmission Modes and the Evolution of Virulence. Evolution. 2001; 55:2389–2400. [PubMed: 11831655]

Day T. Virulence evolution and the timing of disease life-history events. Trends in Ecology & Evolution. 2003; 18:113–118.

Day, T.; Gandon, S. Insights from Price's equation into evolutionary epidemiology. In: Feng, Z.; Dieckmann, U.; Levin, S., editors. Disease evolution: models, concepts and data analyses. Vol. 71. American Mathematical Society; 2006. p. 23-43.DIMACS Series in Discrete Mathematics and Theoretical Computer Science

Day T. Applying population-genetic models in theoretical evolutionary epidemiology. Ecology Letters. 2007; 10:876–888. [PubMed: 17845288]

Day T, Proulx SR. A general theory for the evolutionary dynamics of virulence. The American naturalist. 2004; 163:40–63.

de Roode JC, Yates AJ, Altizer S. Virulence-transmission trade-offs and population divergence in virulence in a naturally occurring butterfly parasite. Proceedings of the National Academy of Sciences. 2008; 105:7489–7494.

Dhondt A, Badyaev A, Dobson A, Hawley D, Driscoll M, Hochachka W, Ley D. Dynamics of Mycoplasmal Conjunctivitis in the Native and Introduced Range of the Host. EcoHealth. 2006; 3:95–102.

Faustino CR, Jennelle CS, Connolly V, Davis AK, Swarthout EC, Dhondt AA, Cooch EG. *Mycoplasma gallisepticum* infection dynamics in a house finch population: seasonal variation in survival, encounter and transmission rate. Journal of Animal Ecology. 2004; 73:651–669.

Frank SA. Models of parasite virulence. Quarterly Review of Biology. 1996; 71:37–78. [PubMed: 8919665]

Grodio JL, Hawley DM, Osnas EE, Ley DH, Dhondt KV, Dhondt AA, Schat KA. Pathogenicity and immunogenicity of three *Mycoplasma gallisepticum* isolates in house finches (*Carpodacus mexicanus*). Veterinary Microbiology. 2012; 155:53–61. [PubMed: 21885217]

Haraguchi Y, Sasaki A. The Evolution of Parasite Virulence and Transmission Rate in a Spatially Structured Population. Journal of Theoretical Biology. 2000; 203:85–96. [PubMed: 10704294]

Hastings A, Cuddington K, Davies KF, Dugaw CJ, Elmendorf S, Freestone A, Harrison S, Holland M, Lambrinos J, Malvadkar U, Melbourne BA, Moore K, Taylor C, Thomson D. The spatial spread of invasions: new developments in theory and evidence. Ecology Letters. 2005; 8:91–101.

Hawley D, Davis A, Dhondt A. Transmission-relevant behaviours shift with pathogen infection in wild house finches (Carpodacus mexicanus). Canadian Journal of Zoology. 2007; 85:752–757.

Hawley DM, Dhondt KV, Dobson AP, Grodio JL, Hochachka WM, Ley DH, Osnas EE, Schat KA, Dhondt AA. Common garden experiment reveals pathogen isolate but no host genetic diversity effect on the dynamics of an emerging wildlife disease. Journal of Evolutionary Biology. 2010; 23:1680–1688. [PubMed: 20561136]

Hawley DM, Osnas EE, Dobson AP, Hochachka WM, Ley DH, Dhondt AA. Parallel Patterns of Increased Virulence in a Recently Emerged Wildlife Pathogen. PLoS Biol. 2013; 11:e1001570. [PubMed: 23723736]

Hawley DM, Sydenstricker KV, Kollias GV, Dhondt AA. Genetic diversity predicts pathogen resistance and cell-mediated immunocompetence in house finches. Biology Letters. 2005; 1:326–329. [PubMed: 17148199]

Hochachka WM, Dhondt AA. Density-dependent decline of host abundance resulting from a new infectious disease. Proceedings of the National Academy of Sciences of the United States of America. 2000; 97:5303–5306. [PubMed: 10792031]

Hosseini PR, Dhondt AA, Dobson AP. Spatial spread of an emerging infectious disease: Conjunctivitis in house finches. Ecology. 2006; 87:3037–3046. [PubMed: 17249229]

Jennelle CS, Cooch EG, Conroy MJ, Senar JC. State-specific detection probabilities and disease prevalence. Ecological Applications. 2007; 17:154–167. [PubMed: 17479842]

Kot M, Lewis MA, Driessche Pvd. Dispersal Data and the Spread of Invading Organisms. Ecology. 1996; 77:2027–2042.

Lambrinos JG. How interactions between ecology and evolution influence contemporary invasion dynamics. Ecology. 2004; 85:2061–2070.

Lee CE. Evolutionary genetics of invasive species. Trends in Ecology & Evolution. 2002; 17:386–391.

Lee CE. Evolution of invasive populations. Proceedings of the National Academy of Sciences USA. 2010; 104:15793–15798.

Lenski RE, May RM. The Evolution of Virulence in Parasites and Pathogens: Reconciliation Between Two Competing Hypotheses. Journal of Theoretical Biology. 1994; 169:253–265. [PubMed: 7967617]

Levin S, Pimentel D. Selection of Intermediate Rates of Increase in Parasite-Host Systems. The American Naturalist. 1981; 117:308–315.

Liu QX, Jin Z. Formation of spatial patterns in an epidemic model with constant removal rate of the infectives. Journal of Statistical Mechanics: Theory and Experiment. 2007; 2007:P05002.

Messinger SM, Ostling A. The Consequences of Spatial Structure for the Evolution of Pathogen Transmission Rate and Virulence. The American Naturalist. 2009; 174:441–454.

Murray, JD. Biomathematics. 3. Vol. 17. Springer; New York: 2002. Mathematical Biology: I. An Introduction.

R Core Team. R: A Language and Environment for Statistical Computing. R Foundation for Statistical Computing; Vienna, Austria: 2013.

Shigesada, N.; Kawasaki, K. Biological Invasions: Theory and Practice. Oxford University Press; 1997. Oxford Series in Ecology and Evolution

Skellam JG. Random Dispersal in Theoretical Populations. Biometrika. 1951; 38:196–218. [PubMed: 14848123]

Smith, GD. Numerical Solution of Partial Differential Equations: Finite Difference Methods. Oxford University Press; 1985.

Soetaert K, Petzoldt T, Setzer RW. Solving Differential Equations in R: Package deSolve. Journal of Statistical Software. 2010; 33:1–25. [PubMed: 20808728]

Travis JMJ, Münkemüller T, Burton OJ. Mutation surfing and the evolution of dispersal during range expansions. Journal of Evolutionary Biology. 2010; 23:2656–2667. [PubMed: 20946371]

Travis JMJ, Münkemüller T, Burton OJ, Best A, Dytham C, Johst K. Deleterious Mutations Can Surf to High Densities on the Wave Front of an Expanding Population. Molecular Biology and Evolution. 2007; 24:2334–2343. [PubMed: 17703053]

Williams PD, Dobson AP, Dhondt KV, Hawley DM, Dhondt AA. Evidence of trade-offs shaping virulence evolution in an emerging wildlife pathogen. Journal of Evolutionary Biology. 2014; 27:1271–1278. [PubMed: 24750277]

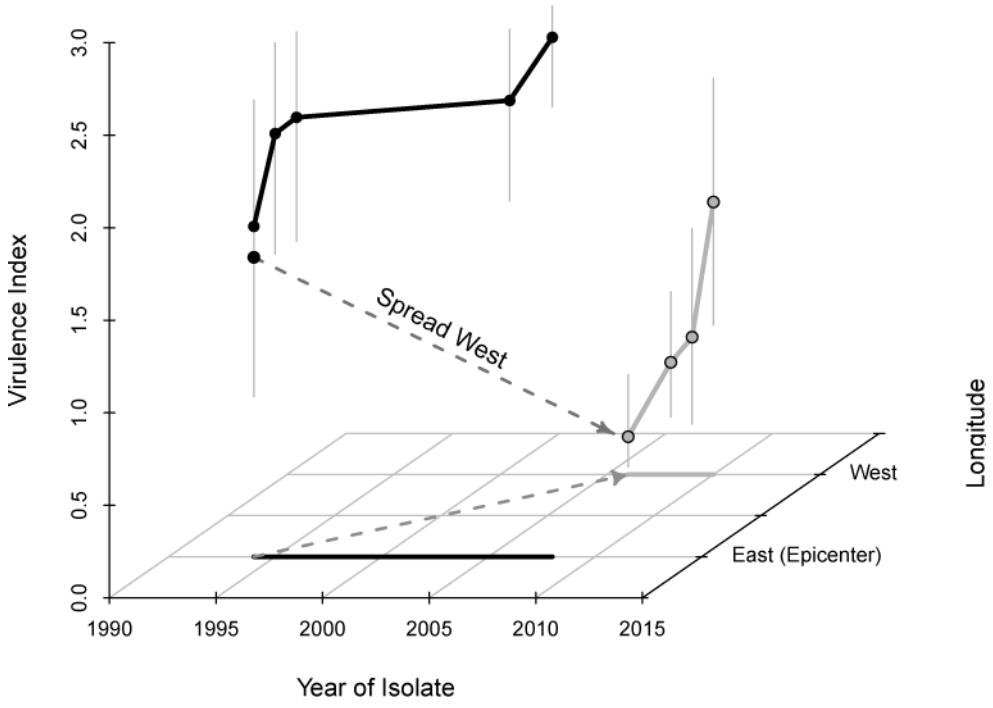

Figure 1.

Virulence dynamics over time in two regions – near the epicenter in eastern North America (black line), and the west coast (gray line) – for the bacterium *Mycoplasma gallisepticum* after its emergence in the House Finch (*Haemorhous mexicanus*). For perspective, the projection of each curve is shown on the Year-Longitude plane. Virulence increases with time at each location, however (see the dashed arrow) there is a large decrease in virulence between the original eastern isolate and the first western isolates. Virulence is measured as the average eye-pathology score post-infection (Hawley et al. 2010). Eastern isolates were collected from finches in eastern North America (Virginia and North Carolina) from the beginning of the outbreak (1994) to 2008. Western isolates were collected in California from when the bacteria was first observed in the state (2006) to 2010. The two points for the 1994 eastern isolate illustrate that host source population (native western, versus introduced eastern, House Finches) has no significant effect on virulence (Hawley et al. 2010). Thin vertical lines are 95% credible intervals for virulence based on experimental details and analytical methods reported in Hawley et al. (2013). The figure here is reproduced from that analysis using the data and R code provided in the online supplement to this article.

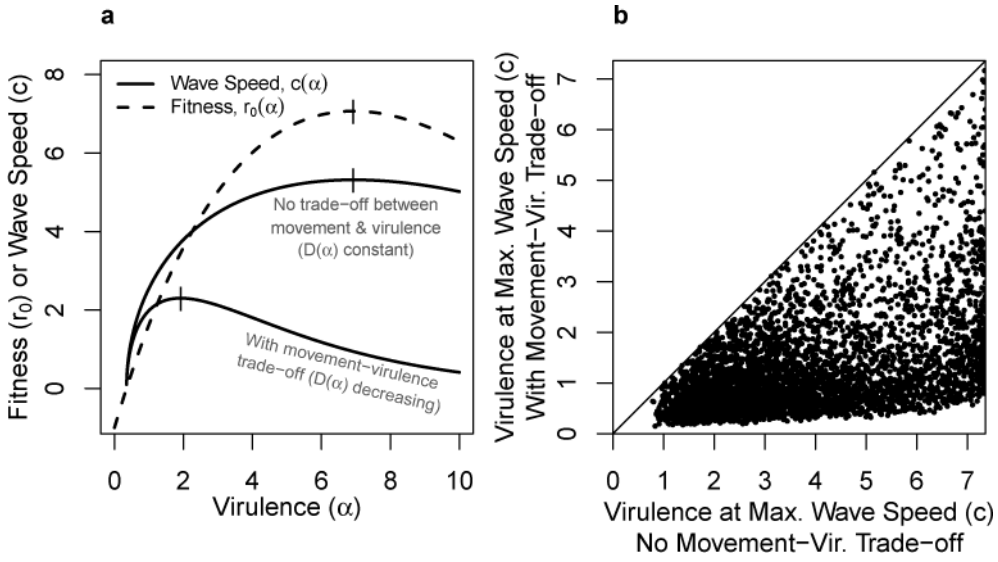

Figure 2.

Simulation results illustrating how the movement-virulence trade-off (equation 8) yields lower virulence levels (α) on the margins of an expanding epidemic. (a) Near the wavefront, selection favors strains with higher wave speeds (i.e., selection maximizes $c(\alpha)$ [solid lines]). Without a movement-virulence trade-off, this is equivalent to maximizing $r_0(\alpha)$ (dashed line). (b) Comparisons of virulence levels that maximize wave speed assuming there is (vertical axis) or there is not (horizontal axis; equivalent to maximizing $r_0(\alpha)$) a movement-virulence trade-off for 5000 combinations of trade-off parameters τ_1 and σ_1. The line is where x-axis values equal y-axis values. Points where all $r(\alpha) < 0$ ($c(\alpha)$ complex numbers) were omitted. Parameters for (a) are $\tau_0 = 0.2$, $\tau_1 = 0.2$, $\sigma_0 = 1$, $\sigma_1 = 0.5$, $\theta = 100$, and $d = 1$. For (b), parameter values for σ_1 and τ_1 were sampled from the range 0–10 by drawing values from the Beta(1,9) distribution and multiplying them by 10 (see the electronic supplement for details).

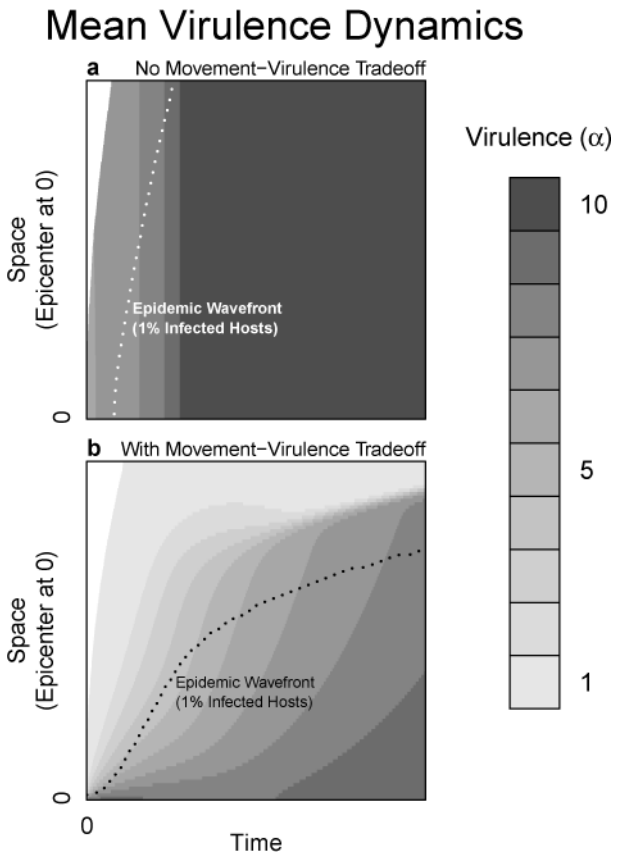

Figure 3.

Mean virulence dynamics across space (vertical axis; distance from the epicenter on a one-dimensional spatial domain) through time (horizontal axis), without (a) and with (b) a movement-virulence trade-off. The white region indicates that total prevalence is very low (below a detection threshold of approximately 10^{-16}), and that the virulence dynamics are not shown. The 'Epidemic Wavefront' line indicates a disease prevalence of 1%. Parameters: In (a) $\sigma_1 = 0$, and in (b) $\sigma_1 = 0.2$. Initial ($x = 0$, $t = 0$) mean virulence and prevalence was set to 5.0 and 1%, respectively. Other parameters are as in Figure 2.

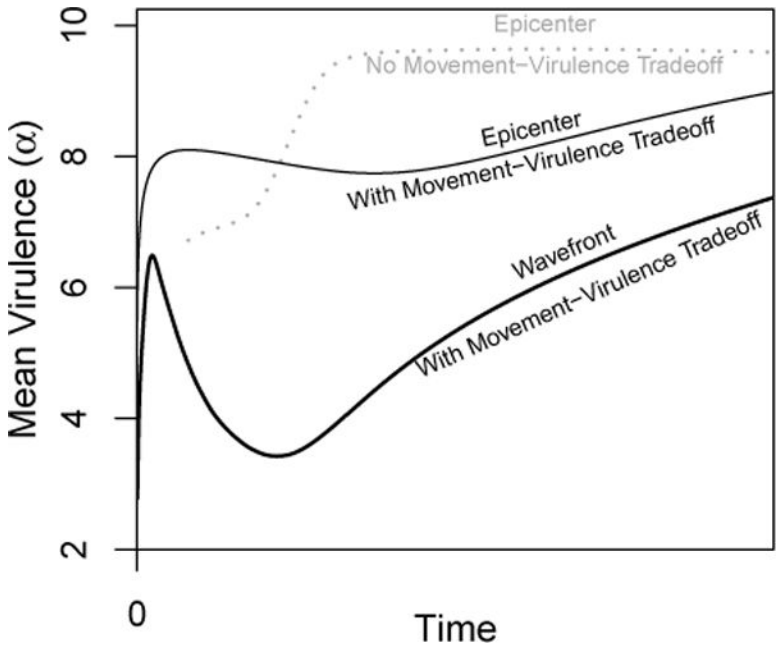

Figure 4.

Comparison of mean virulence changes over time for the epicenter with no host movement trade-off (gray, dotted curve; the wave front virulence dynamics are identical), and for both the epicenter (solid line) and wavefront (bold solid line) for the case with a movement-virulence trade-off. Parameters are the same as in Figure 3.